Pathway of Membrane Fusion with Two Tension-Dependent Energy Barriers

Andrea Grafmüller, Julian Shillcock, and Reinhard Lipowsky
*Max Planck Institute of Colloids and Interfaces, Science Park Golm, 14424 Potsdam, Germany**
(Received 2 February 2007; published 23 May 2007)

Fusion of bilayer membranes is studied via dissipative particle dynamics (DPD) simulations. A new set of DPD parameters is introduced which leads to an energy barrier for flips of lipid molecules between adhering membranes. A large number of fusion events is monitored for a vesicle in contact with a planar membrane. Several time scales of the fusion process are found to depend exponentially on the membrane tension. This implies an energy barrier of about $10k_BT$ for intermembrane flips and a second size-dependent barrier for the nucleation of a small hemifused membrane patch.

DOI: 10.1103/PhysRevLett.98.218101 PACS numbers: 87.16.Dg, 61.20.Ja

Introduction.—Fusion of biological membranes is an essential process in many areas of cell biology, from viral fusion to vesicular trafficking and synaptic transmission [1]. Biological membranes are complex systems composed of many different lipids and proteins. For a better understanding of the fundamental processes involved, lipid membranes are often used as simplified model systems [2]. Even in the absence of proteins, the fusion of lipid membranes and vesicles can be experimentally induced by a variety of fusogenic agents such as membrane tension, electroporation, or adsorption of Ca^{++} ions. For both biomembranes and lipid bilayers, the early stages of fusion are believed to lead to the formation of a fusion pore, i.e., a necklike connection between the two bilayers, with an initial size of about 10 nm. The corresponding time scale has not been measured, but both patch clamp methods applied to synaptic membranes [3] and ultrafast optical microscopy of giant vesicles [4] indicate that the fusion pore can be formed in less than 100 μs.

Since it is currently not possible to resolve these length and time scales experimentally, computer simulations such as Brownian dynamics [5], Monte Carlo simulations [6], coarse-grained molecular dynamics (MD) [7–9], dissipative particle dynamics (DPD) [10,11], atomistic MD [12], and Markovian state models based on coarse-grained MD [13] have been used to obtain insight into the process of fusion pore formation. Here, we focus on the presumably simplest way to induce lipid bilayer fusion, namely, via membrane tension, which is coupled to hydrodynamics and can be directly controlled in MD [14] and DPD [10,15] simulations with explicit water, see Fig. 1.

The experimentally observed frequency of fusion events increases with osmotic inflation of the vesicles [16] which indicates that the energy barriers for fusion can be reduced by increasing membrane tension. This mechanism will be elucidated in the present Letter, in which we report the first measurements of these barriers by computer simulations. In fact, we find that the formation of the fusion pore is governed by two successive barriers in contrast to the various ''stalk'' models, reviewed in [2], that are based on elastic theories for membrane sheets and advertise the idea of a single energy barrier.

The fusion statistics observed in previous DPD simulations [10] did not indicate any tension-dependent energy barriers. Further studies of the corresponding set of DPD parameters showed that this set is characterized by fast flips of lipid molecules between adhering membranes. In contrast, the present study is based on a new set of DPD parameters, for which these lipid flips have to overcome an energy barrier that depends on membrane tension and contributes to the total barrier for membrane fusion.

Our fusion geometry consists of a vesicle with a diameter of 15 or 30 nm in contact with a planar membrane with

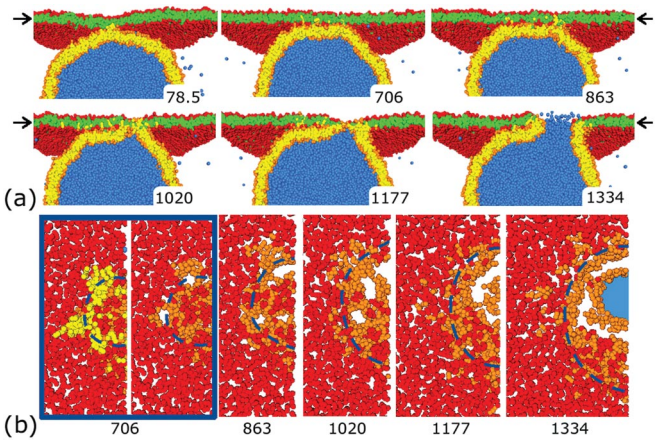

FIG. 1 (color). Fusion of a vesicle (yellow + orange) with a diameter of 30 nm to a planar membrane (green + red) with a linear size of 50 nm. The vesicle consists of 6869 lipids with orange heads and yellow chains (or tails). The planar membrane contains 6911 lipids with red heads and green chains. The water beads initially inside and outside the vesicle are blue and transparent, respectively. (a) Six successive snapshots, side view, from 78.5 ns up to 1334 ns after initial contact. Lipids start to undergo interbilayer flips along the contact line after 78.5 ns. This leads to a disordered bean-shaped region in which a small hemifused membrane patch nucleates at about 1177 ns. (b) The same membrane conformations viewed in a plane parallel to the planar membrane as indicated by the arrows in (a). The blue broken line corresponds to the contact line.

an area of $(50\ \mathrm{nm})^2$, see Fig. 1, which shows one successful fusion event of a 30 nm vesicle. In this example, the vesicle spreads onto the planar membrane and forms a relatively sharp contact angle after 706 ns, see Fig. 1(a). During the spreading process, the lipids start to flip from the vesicle into the planar membrane after 78.5 ns. This flipping process, which is localized along the contact line, leads to the formation of a bean-shaped, partially fused, and highly disordered membrane domain within the contact zone, see Fig. 1(b). Finally, an ordered hemifused bilayer patch appears in the middle of the bean-shaped domain and then ruptures to form the fusion pore after about 1334 ns.

Figure 1 represents one example of the time evolution of more than 140 fusion attempts that we have simulated and analyzed. We used the initial tensions of the membranes as control parameters that were changed by varying the projected areas per lipid. In contrast to the DPD parameters used in Ref. [10], the new parametrization used here leads to fusion times that depend strongly on the initial tension. A detailed analysis of this dependence shows that the observed fusion process is governed by two successive energy barriers: a first barrier for the interbilayer flips of lipid molecules and a second one for the nucleation of an ordered hemifused bilayer patch.

Our Letter is organized as follows. First, we briefly review the DPD simulation method and our membrane models. Second, we discuss the qualitative features of the different pathways observed after initial contact between vesicle and planar membrane. Third, we describe our quantitative results about the dependence of the fusion statistics on the initial membrane tension. Finally, the observed fusion times are analyzed and shown to involve two tension-dependent energy barriers.

Simulation method.—The DPD model explicitly includes water, reproduces the correct hydrodynamics [17,18], and can be used to explore the self-assembly and phase behavior of lipid molecules in water [15,19,20]. The DPD particles or beads represent small fluid volumes rather than single atoms or molecules, so that their interaction potentials become softly repulsive and short ranged, see Appendix A in [21]. All potentials are taken to have the same range r_o but their amplitudes a_{ij} differ for different bead species. We use three different species of beads: head (H), chain (C), and water (W) beads. Each lipid molecule consists of a headgroup with three H beads and two chains with 2×4 C beads as in [10,14]. This architecture corresponds to the phospolipid dimyristoylphosphatidylcholine (DMPC), see Appendix A in [21].

It is generally believed that the hydration of lipids acts to stabilize membrane adhesion and to prevent their fusion. This implies that, in the absence of membrane tension, intermembrane flips of lipid molecules experience a substantial energy barrier which should correspond to the hydration energy of a single chain or of a splayed lipid configuration with one chain inserted in each membrane (the latter configuration has been observed both in coarse-grained [8] and all-atom molecular dynamics simulations [12]). The hydration energy for a fully hydrated DMPC molecule is about $23.8 k_B T$ as can be estimated from the functional dependence of the critical micelle concentration on the chain length [22]. One thus expects an energy barrier $\Delta E_{\alpha,0}$ of the order of $10 k_B T$ for flips between two adhering DMPC membranes.

For our coarse-grained model of DMPC, we have determined this barrier by simulating the following process. Starting from two adhering planar membranes in their tensionless state, a single C bead was pulled slowly by an external force until the corresponding lipid assumed the aforementioned splayed configuration with one chain inserted in each membrane. We measured the average work performed during this process which provides an estimate for the energy barrier $\Delta E_{\alpha,0}$. For the new DPD parameter set used here, we found that $\Delta E_{\alpha,0} = 9 \pm 2 k_B T$.

In addition, the new parameter set leads to an essentially linear relationship between the (projected) molecular area A of the lipid molecules in the planar membrane and the membrane tension Σ, see Appendix B in [21]. It is convenient to define the dimensionless molecular area $\bar{A} \equiv A/r_o^2$ and the dimensionless tension $\bar{\Sigma} \equiv \Sigma r_o^2/k_B T$. The stress-strain relationship then has the simple form $\bar{\Sigma} = \bar{K}_A(\bar{A} - \bar{A}_0)/\bar{A}_0$ with the dimensionless modulus $\bar{K}_A = 18.2$ and the molecular area $\bar{A}_0 = 1.25$ of the tensionless state.

The vesicle is assembled within a spherical shell close to the planar membrane, see Appendix C in [21]. The initial molecular area $\bar{A}$ of the planar membrane is controlled by varying the number of lipids for constant size of the simulation box, which is a cuboid with a base area of $(50\ \mathrm{nm})^2$. The box height is taken to be 35 and 50 nm for vesicles with a diameter of 15 and 30 nm, respectively. The basic length scale is obtained from the molecular area of the DMPC lipids and the basic time scale from their in-plane diffusion constant, see Appendix A in [21].

Fusion process and alternative pathways.—Using this fusion protocol, we have monitored more than 140 fusion attempts between vesicle and planar membranes. Initially, the vesicle spreads onto the planar membrane and adheres to it. This spreading process increases the tension of the vesicle membrane since this membrane develops a roughly planar contact area whereas the vesicle volume stays essentially constant. While the contact area is growing, lipids close to the contact line start to undergo interbilayer flips from the vesicle into the planar membrane. The flipping chains force the head beads to move apart, strongly perturbing the local bilayer structure.

These interbilayer flips lead to a bean-shaped, partially fused membrane domain characterized by intermingling of the lipids and direct contact of the hydrophobic cores of the two bilayers. This rearrangement is initiated at the contact line because (i) the vesicle membrane has a pronounced "kink" of high curvature along this line and (ii) the vesicle lipids are already tilted with respect to the planar membrane so that the necessary rotational displacement for the

flips is reduced. The partially fused membrane domain grows along the contact line, while the lipids in its center again assume a more ordered state corresponding to a hemifused bilayer patch. This bilayer patch grows for a relatively short time, typically between 150 and 300 ns, before it ruptures to form the final fusion pore.

All successful fusion events involve the same membrane conformations, differing mainly in the times needed for the different intermediate steps. Especially the duration of the adhering state varies greatly and depends strongly on the initial tension $\bar{\Sigma}$. For relatively large $\bar{\Sigma}$, the fusion process starts on first contact, whereas for small $\bar{\Sigma}$, lipid exchange between the membranes is slowed down leading to large contact areas and long adhesion times.

Fusion is not the only relaxation pathway. Alternative outcomes are (meta)stable adhesion or hemifusion for low molecular area $\bar{A}$ and rupture of tense membranes. If the initial value of $\bar{A}$ is only slightly larger than $\bar{A}_0$ corresponding to $\bar{\Sigma} = 0$, the contact area grows until the system reaches a mechanical equilibrium state, for which the forces along the contact line are balanced. This state is characterized by a small rate of interbilayer flips.

Fusion statistics.—Despite these alternative pathways, the majority of fusion attempts leads to fusion for the bilayer membranes studied here. For the 15 and 30 nm vesicles, 55 out of 83 and 40 out of 62 fusion attempts were successful, respectively. The frequencies of the different pathways are given in Appendix C in [21].

As far as the vesicle size is concerned, we observe several qualitative differences between the fusion processes of the larger and smaller vesicles. For $\bar{A} = 1.4$, for example, most 15 nm vesicles fused within 4 μs whereas we did not observe any fusion of 30 nm vesicles up to 12 μs. For the unsuccessful fusion attempts, the smaller and larger vesicles preferentially attained hemifused and adhering states, respectively. This can be understood from a balance between adhesion and elastic energies which dominate for large and small vesicles, respectively.

In addition to the success rate, the tension of the planar membrane also determines the fusion time, t_{fu}, which is the time from the first contact between planar membrane and vesicle until the opening of the fusion pore. The cumulative histograms for the observed fusion times of the 30 nm and 15 nm vesicles are displayed in Fig. 2(a) and 2(b), respectively. The different colors used in these histograms correspond to different molecular areas $\bar{A}$ of the planar membrane whereas the different shades of each color reflect the molecular area $\bar{A}_{\mathrm{ve}}$ of the vesicle membrane.

Long fusion times correspond to vesicles that attain an intermediate adhering state in mechanical equilibrium. Thus, it is rather likely that some of the events that were observed to stay in the adhering state up to 12 μs will eventually fuse on longer time scales. Figure 2 also shows that the fusion time distribution is shifted towards larger values and attains a larger width as one decreases the initial area and, thus, the membrane tension.

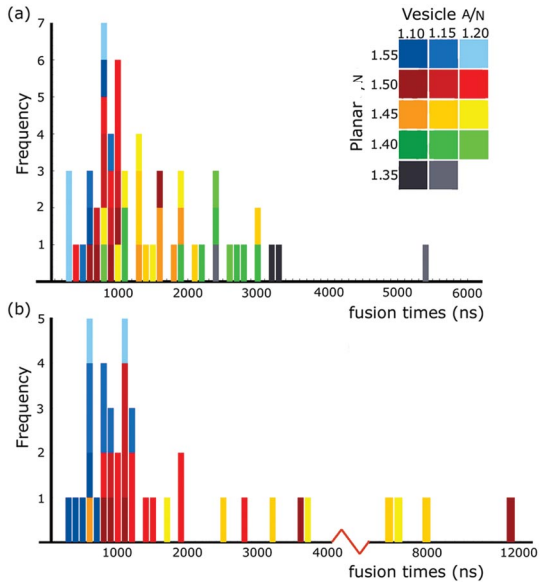

FIG. 2 (color). Cumulative histograms of observed fusion times for (a) 15 nm and (b) 30 nm vesicle. Color code: violet, red, yellow, green, and gray correspond to initial molecular area $\bar{A} = 1.55$, 1.55, 1.45, 1.4, and 1.35 of the planar membrane. Different shades of each color correspond to different molecular areas $\bar{A}_{\mathrm{ve}}$ of the vesicle membrane, see inset in the right upper corner. The clear separation of the colors reflects the strong dependence of the average fusion time on membrane tension. Histogram (b) is rather broad with a fat tail; the very long fusion times reflect the increased stability of the adhering state.

Fusion times and energy barriers.—The data for the average fusion time $\langle t_{\mathrm{fu}} \rangle$ and for the width $\Delta t_{\mathrm{fu}} \equiv \sqrt{\langle (t_{\mathrm{fu}} - \langle t_{\mathrm{fu}} \rangle)^2 \rangle}$ of the fusion time distribution are displayed in Fig. 3. Inspection of this figure shows that both time scales decay exponentially with increasing $\bar{A} - \bar{A}_0$, where $\bar{A}_0 = 1.25$ is the molecular area of the tensionless state as before. Using the linear dependence of tension $\bar{\Sigma}$ on $\bar{A} - \bar{A}_0$, see Appendix B in [21], the average fusion time is found to behave as $\langle t_{\mathrm{fu}} \rangle = t_{\mathrm{fu},0} \exp(-\bar{A}_* \bar{\Sigma})$ with $t_{\mathrm{fu},0} \simeq 9.0$ μs and $\bar{A}_* \simeq 0.52$ for the 15 nm vesicle as well as

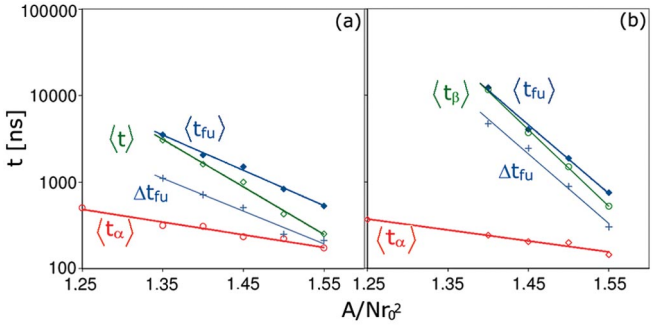

FIG. 3 (color). Various time scales that characterize the fusion process as functions of the dimensionless molecular area $A/Nr_o^2 = \bar{A}$ for (a) 15 nm and (b) 30 nm vesicles: average fusion time $\langle t_{\mathrm{fu}} \rangle$, average first flipping time $\langle t_\alpha \rangle$, average reordering time $\langle t_\beta \rangle$, and width Δt_{fu} of fusion time distribution.

$t_{fu,0} \simeq 178\ \mu s$ and $\bar{A}_* \simeq 1.0$ for the 30 nm vesicle. Since both the average fusion time $\langle t_{fu} \rangle$ and the width Δt_{fu} grow exponentially as one reduces the tension, it becomes exceedingly difficult to determine these time scales as one approaches the tensionless state.

In order to further analyze the functional dependence of the fusion time on the tension Σ, we decompose the fusion process into three subprocesses. (i) Subprocess α consists of the adhesion process from the first contact between the two bilayers up to the time when the first lipid molecules flip from the vesicle to the planar membrane. The duration of this process defines the first flipping time t_α. (ii) Subprocess β consists of the intermingling and partial fusion process starting with the first interbilayer flip up to the nucleation of the ordered hemifused patch. The duration of this second process defines the reordering time t_β. (iii) Subprocess γ corresponds to the rupture of the hemifused patch which leads to the fusion pore. By definition, the total fusion time $t_{fu} = t_\alpha + t_\beta + t_\gamma$.

For process α, the hydrated lipid head groups of the well-ordered bilayers provide an energy barrier, ΔE_α, for the flips of the lipid chains. For vanishing tension, the corresponding energy barrier should be comparable to $\Delta E_{\alpha,0} = (9 \pm 2) k_B T$ as measured directly for two adhering planar membranes. This energy barrier should be reduced with increasing tension Σ since such an increase moves the head groups in the planar membrane further apart. Thus, the dimensionless barrier $\Delta \bar{E}_\alpha \equiv \Delta E_\alpha / k_B T$ should have the functional form $\Delta \bar{E}_\alpha = \Delta \bar{E}_{\alpha,0} - \bar{A}_\alpha \bar{\Sigma}$ with a characteristic area $\bar{A}_\alpha$, and the average value, $\langle t_\alpha \rangle$, of the first flipping time should behave as $\langle t_\alpha \rangle = t_{sc} \exp[\Delta \bar{E}_{\alpha,0} - \bar{A}_\alpha \bar{\Sigma}]$. Such an exponential decay of $\langle t_\alpha \rangle$ with increasing tension is indeed observed in our simulations with $\bar{A}_\alpha \simeq 0.19$ and 0.16 for the 15 nm and the 30 nm vesicles, respectively, see Fig. 3.

It is also plausible that the nucleation of an ordered bilayer patch within the disordered, partially fused membrane domain is a thermally activated process. The corresponding energy barrier should have the analogous form $\Delta \bar{E}_\beta = \Delta \bar{E}_{\beta,0} - \bar{A}_\beta \bar{\Sigma}$, where $\Delta \bar{E}_{\beta,0}$ is the energy barrier for the process β at zero tension and $\bar{A}_\beta$ another characteristic area. The average reordering time should then behave as $\langle t_\beta \rangle = t_{sc} \exp[\Delta \bar{E}_{\beta,0} - \bar{A}_\beta \bar{\Sigma}]$. Such an exponential decay of $\langle t_\beta \rangle$ with increasing tension Σ is again observed in our simulations with $\Delta \bar{E}_{\beta,0} = 12.1 \pm 2$ and 15.5 ± 2 as well as $\bar{A}_\beta \simeq 0.69$ and 1.12 for the 15 nm and the 30 nm vesicles, respectively, see Fig. 3. Because of the exponential Σ dependence of both $\langle t_\alpha \rangle$ and $\langle t_\beta \rangle$, an improved fit to the average fusion time $\langle t_{fu} \rangle$ consists of two superimposed exponentials.

Summary.—In summary, we have introduced a new set of DPD parameters for which the intermembrane flips of lipid molecules represent a thermally activated process. These bilayer membranes exhibit a fusion pathway that is governed both by the energy barrier for intermembrane flips and by a second barrier for the nucleation of a small hemifused membrane segment. The corresponding fusion times increase exponentially with decreasing tension as displayed in Fig. 3. It would be highly desirable to obtain experimental data on intermembrane flips and the corresponding energy barrier ΔE_α for a specific lipid such as DMPC. We could then further optimize the DPD parameters in order to match the measured value of this barrier and, thus, to predict the fusion statistics for this lipid species in a quantitative manner.

We thank Reinhard Jahn and Lianghui Gao for stimulating discussions.

*Electronic address: www.mpikg.mpg.de/theory/

[1] R. Jahn, T. Lang, and T. C. Südhof, Cell **112**, 519 (2003).
[2] L. K. Tamm, J. Crane, and V. Kiessling, Current Opinion Struct. Biol. **13**, 453 (2003).
[3] M. Lindau and G. A. de Toledo, Biochim. Biophys. Acta **1641**, 167 (2003).
[4] C. K. Haluska, K. A. Riske, V. Marchi-Artzner, J.-M. Lehn, R. Lipowsky, and R. Dimova, Proc. Natl. Acad. Sci. U.S.A. **103**, 15 841 (2006).
[5] H. Noguchi and M. Takasu, J. Chem. Phys. **115**, 9547 (2001).
[6] M. Müller, K. Katsov, and M. Schick, J. Chem. Phys. **116**, 2342 (2002).
[7] S. J. Marrink and A. E. Mark, J. Am. Chem. Soc. **125**, 11 144 (2003).
[8] M. J. Stevens, J. H. Hoh, and T. B. Woolf, Phys. Rev. Lett. **91**, 188102 (2003).
[9] K. Pieterse, A. F. Smeijers, A. J. Markvoort, and A. J. Hilbers, J. Phys. Chem. B **110**, 13 212 (2006).
[10] J. Shillcock and R. Lipowsky, Nat. Mater. **4**, 225 (2005).
[11] D. W. Li and X. Y. Liu, J. Chem. Phys. **122**, 174909 (2005).
[12] V. Knecht, A. E. Mark, and S.-J. Marrink, J. Am. Chem. Soc. **128**, 2030 (2006).
[13] P. M. Kasson, N. W. Kelley, N. Singhal, M. Vrjic, A. T. Brunger, and V. S. Pande, Proc. Natl. Acad. Sci. U.S.A. **103**, 11 916 (2006).
[14] R. Goetz and R. Lipowsky, J. Chem. Phys. **108**, 7397 (1998); R. Goetz, G. Gompper, and R. Lipowsky, Phys. Rev. Lett. **82**, 221 (1999).
[15] J. C. Shillcock and R. Lipowsky, J. Chem. Phys. **117**, 5048 (2002).
[16] A. Finkelstein, J. Zimmerberg, and F. S. Cohen, Annual Review of Physiology **48**, 163 (1986).
[17] R. D. Groot and P. B. Warren, J. Chem. Phys. **107**, 4423 (1997).
[18] I. Vattulainen, M. Karttunen, G. Besold, and J. M. Polson, J. Chem. Phys. **116**, 3967 (2002).
[19] S. Yamamoto, Y. Maruyama, and S.-A. Hyodo, J. Chem. Phys. **116**, 5842 (2002).
[20] M. Kranenburg, M. Venturoli, and B. Smit, Phys. Rev. E **67**, 060901 (2003).
[21] See EPAPS Document No. E-PRLTAO-98-029720 for supplementary material. For more information on EPAPS, see http://www.aip.org/pubservs/epaps.html.
[22] G. Cevc and D. Marsh, *Phospholipid Bilayers: Physical Principles and Models* (Wiley, New York, 1987).